Chinese Chemical Letters 35 (2024) 108536

Contents lists available at ScienceDirect

Chinese Chemical Letters

journal homepage: www.elsevier.com/locate/cclet

Tumor-targeted self-assembled micelles reducing PD-L1 expression combined with ICIs to enhance chemo-immunotherapy of TNBC

Hongda Zhu[a,1,*], Kai Ma[a,1], Rui Ruan[a], Chaobo Yang[a], Aqin Yan[a], Jing Li[b], Qi Yu[a,c], Hongmei Sun[a], Mingxing Liu[a], Hongmei Zheng[b], Jing Gao[d], Xiaofang Guan[e], Zhu Dai[b,*], Yao Sun[c,*]

[a] *Cooperative Innovation Center of Industrial Fermentation (Ministry of Education & Hubei Province), Key Laboratory of Fermentation Engineering (Ministry of Education), National "111" Center for Cellular Regulation and Molecular Pharmaceutics, School of Food and Biological Engineering, Hubei University of Technology, Wuhan 430068, China*
[b] *Hubei Cancer Hospital, Tongji Medical College, Huazhong University of Science and Technology, Wuhan 430079, China*
[c] *National Key Laboratory of Green Pesticide, College of Chemistry, Central China Normal University, Wuhan 430079, China*
[d] *Key Laboratory of Medical Optics, Suzhou Institute of Biomedical Engineering and Technology, Chinese Academy of Sciences, Suzhou 215163, China*
[e] *Key Laboratory of Optic-electric Sensing and Analytical Chemistry for Life Science, Ministry of Education, Qingdao University of Science and Technology, Qingdao 266000, China*

ARTICLE INFO

Article history:
Received 7 February 2023
Revised 29 April 2023
Accepted 5 May 2023
Available online 6 May 2023

Keywords:
Immunotherapy
Tumor-targeted
Self-assembled micelles
Metformin
Reducing PD-L1 expression
TNBC

ABSTRACT

Immune checkpoint inhibitors (ICIs) therapy targeting programmed cell death ligand 1 (PD-L1) and programmed death protein 1 (PD-1) had exhibited significant clinical benefits for cancer treatment such as triple negative breast cancer (TNBC). However, the relatively low anti-tumor immune response rate and ICIs drug resistance highlight the necessity of developing ICIs combination therapy strategies to improve the anti-tumor effect of immunotherapy. Herein, the immunomodulator epigallocatechin gallate palmitate (PEGCG) and the immunoadjuvant metformin (MET) self-assembled into tumor-targeted micelles *via* hydrogen bond and electrostatic interaction, which encapsulated the therapeutic agents doxorubicin (DOX)-loaded PEGCG-MET micelles (PMD) and combined with ICIs (anti-PD-1 antibody) as therapeutic strategy to reduce the endogenous expression of PD-L1 and improve the tumor immunosuppressive microenvironment. The results presented that PMD integrated chemotherapy and immunotherapy to enhance antitumor efficacy *in vitro* and *in vivo*, compared with DOX or anti-PD-1 antibody for the therapy of TNBC. PMD micelles might be a potential candidate, which could remedy the shortcomings of antibody-based ICIs and provide synergistic effect to enhance the antitumor effects of ICIs in tumor therapy.

Immunotherapy represented by immune checkpoint inhibitors (ICIs) has become a significant therapy for tumors. However, tumor-induced immunosuppression and low effective anti-tumor immune response were the main challenges for ICIs immunotherapy [1]. For example, antibody-based ICIs block programmed cell death ligand 1 (PD-L1) and programmed death protein 1 (PD-1) binding through structural blocking PD-L1 on cancer cell surface, but the effect might be attenuated by the active redistribution of intracellular PD-L1 to the cell membrane, causing impaired anticancer effects [2,3]. In addition, the lack of tumor-infiltrating T lymphocytes and the presence of immunosuppressive microenvironment also impeded the treatment of tumors with ICIs, such as myeloid-derived suppressor cells (MDSCs) and regulatory T cells (Tregs) could inhibit antibody-based ICIs-regenerated anti-tumor toxic T lymphocyte responses [4]. Therefore, it was particularly important to develop the strategy of ICIs combination therapy to reduce the endogenous expression of PD-L1 and remodel the antitumor effect of ICIs.

In recent years, some chemotherapeutics for instance doxorubicin (DOX), mitoxantrone and cyclophosphamide had been found to evoke immunogenic cells death (ICD), which could improve tumor immune microenvironment, promote dendritic cell (DC) maturation and enhance anti-tumor effects [5,6]. Epigallocatechin gallate palmitate (PEGCG) was an acylation product formed by the chemical reaction between epigallocatechin gallate (EGCG) and palmitoyl chloride, but it retained the original biological activity of EGCG. In addition to its anti-inflammatory, antioxidant and anti-

* Corresponding authors.
E-mail addresses: bszzhuhongda@yeah.net (H. Zhu), daizhu_1226@sina.com (Z. Dai), sunyaogbasp@ccnu.edu.cn (Y. Sun).
[1] These authors contributed equally to this work.

https://doi.org/10.1016/j.cclet.2023.108536
1001-8417/

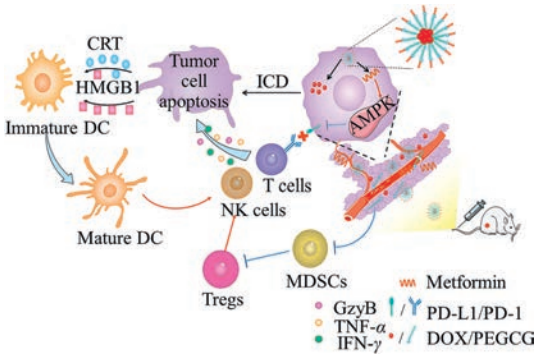

Scheme 1. Illustration of self-assembled micelles PMD to reduce PD-L1 expression and enhance chemo-immunotherapy.

tumor effects, EGCG could further inhibit Tregs by inducing apoptosis of MDSCs, thereby remodeling the tumor immunosuppressive microenvironment [7]. Besides, EGCG had a high affinity to laminin receptors which were highly expressed in cancer cells such as breast cancer cells [8]. Metformin (MET) as a prevalent drug for the treatment of type 2 diabetes had been found many new functions such as curbing tumor progression [9] and reducing the expression of PD-L1 to promote the antitumor immunity [10]. Hence, MET as an immunoadjuvant might provide a new approach to solve the dilemma faced by immune checkpoint therapy [11].

TNBC was a troublesome subtype of breast cancer with a high rate of metastasis and recurrence. Under a single-modality therapy, its treatment was usually difficult to produce long-term and effective therapeutic effects [12]. ICIs had been largely explored in the field of breast cancer, and might be a useful treatment strategy for TNBC [13]. However, the cancer intracellular expression of PD-L1 and different tumor immune escape mechanisms might impair the therapeutic benefits of ICIs [14].

To validate the above hypothesis, we constructed a tumor-targeted self-assembled micelle to enhance antitumor efficacy through combining immunotherapy and chemotherapy. As displayed in Scheme 1, the immunomodulatory PEGCG and the immunoadjuvant MET were self-assembled into micelles *via* hydrogen bond and electrostatic interaction, and were denoted as PEGCG-MET micelles (PM) micelles. PM micelles were used to encapsulate the therapeutic agents DOX, denoted as DOX-loaded PM micelles (PMD) micelles. Different from traditional ICIs blocking PD-L1 on the cancer cell membrane, PMD micelles could directly inhibit the endogenous expression of PD-L1. When PMD micelles were combined with ICIs (such as anti-PD-1 antibody) as therapeutic strategy, it displayed stronger anticancer effect both *in vitro* and *in vivo* compared with DOX or anti-PD-1 antibody, which could remedy the shortcomings of antibody-based ICIs and provide synergistic effect to enhance the antitumor effects of ICIs in tumor therapy.

In this work, PMD nanoparticles were facilely prepared by self-assembled approach. In detail, PEGCG with negatively charged phenolic hydroxyl group and MET with positively charged amino group could self-assemble to form PM micelles based on hydrogen bonds and electrostatic interaction. PM and PMD micelles could be well dispersed with an average hydrated particle size of about 180 nm and 200 nm (Fig. 1A). Compared to PM, the increase in particle size of PMD was related to DOX (a hydrophobic drug) loaded. DOX could enter the hydrophobic core of the micelles through hydrophobic interaction, increasing the volume of the core and enhancing the structural stability of the micelles. Transmission electron microscope (TEM) images presented a regular circular shape with an average particle size of 190 nm (Fig. 1B). Due to the positive charge of DOX, zeta potentials of PM and PMD were from −29 mV to −23 mV, respectively (Fig. 1C). Ultraviolet (UV) absorption peak of PM micelles showed a clear blue shift compared with P/M (Fig. 1D), which might be ascribed to π-π stacking in PM micelles, resulting in π orbital energy decreased and π^* orbital energy increased, thereby shifting the UV absorption to shorter wavelengths. Fourier transform infrared spectroscopy was used to further verify the self-assembly of PM micelles (Fig. S1 in Supporting information). As detected by fluorescence spectrophotometer, the encapsulation efficiency and loading capacity of PMD based on the Standard curve of DOX were 74.8% and 15.7%, respectively. PMD micelles showed obvious sustained release effect, compared with free DOX, which greatly reduced the release rate of DOX, thereby avoiding peak and valley phenomena in blood concentration, reducing the toxic and side effects of DOX while prolonging its blood circulation time (Fig. 1E). The particle size and polydispersity index (PDI) of PMD micelles did not show significantly changes within 60

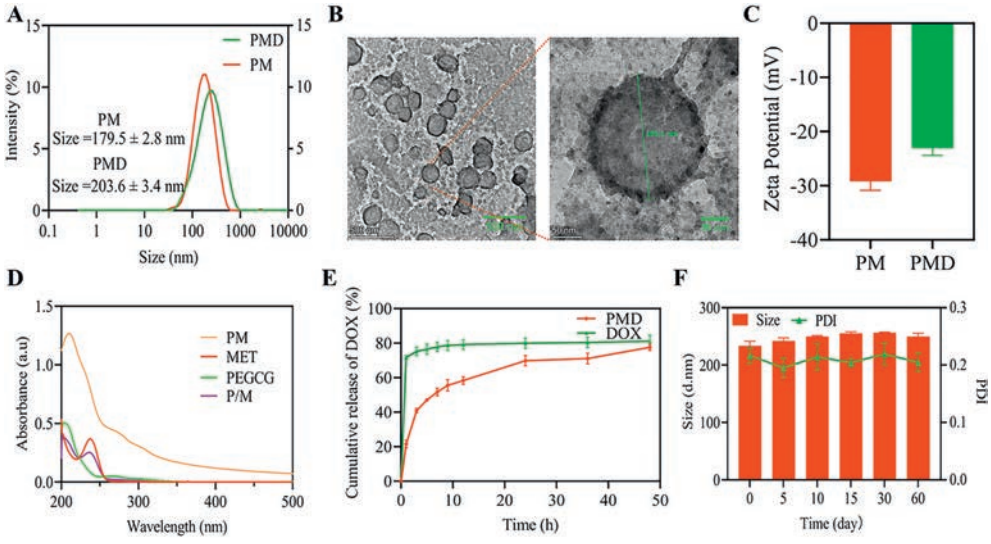

Fig. 1. Characterization of self-assembled micelles. (A) Dynamic light scattering (DLS) measurement of PM and PMD micelles. (B) TEM image of PMD micelles, Scale bars: 500 nm and 50 nm. (C) Zeta potential of PM and PMD micelles. (D) Ultraviolet–visible spectrophotometry (UV–vis) absorption spectra of PM, MET, PEGCG and PEGCG/MET mixture (P/M). (E) *In vitro* release behavior of PMD micelles and DOX solution in PBS at 37 °C. (F) Changes in particle size and PDI of PMD micelles within 60 days. Data were shown as mean ± standard deviation (SD) ($n = 3$).

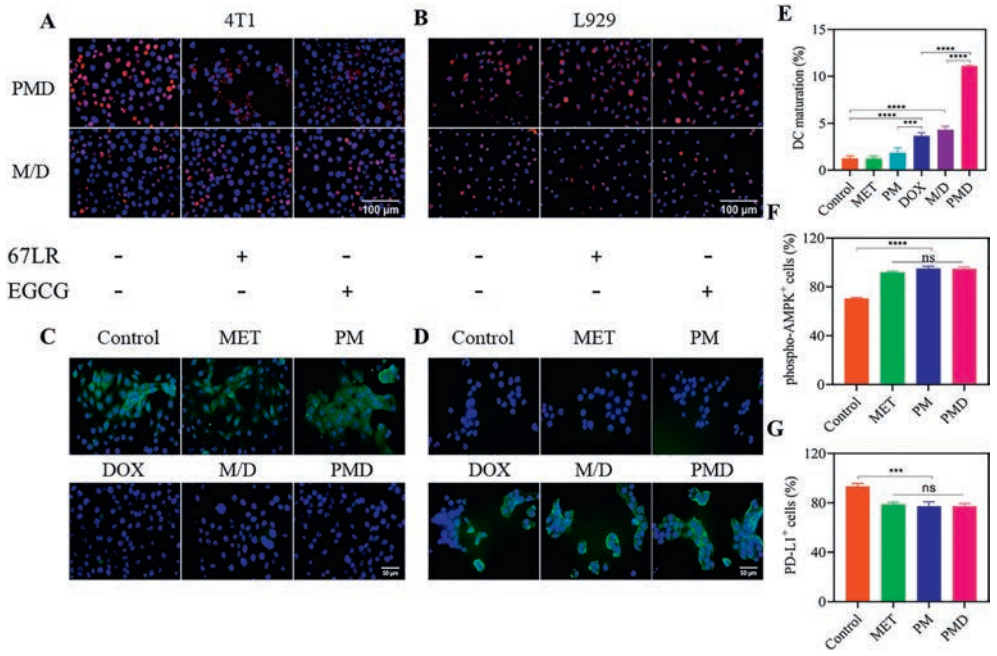

Fig. 2. Cellular targeting assay and ICD induced by PMD micelles *in vitro*. (A) Uptake of PMD micelles (upper line) and M/D (down line) by 4T1 cells and (B) L929 cells after blocking agent treatment, Scale bar: 100 μm. (C) Immunofluorescent staining examination of HMGB1 release in 4T1 cells and (D) CRT exposure on the surface of 4T1 cells treated with different groups, Scale bar: 50 μm. (E) Quantitation of DC maturation. (F) Quantitative examination of p-AMPK and (G) PD-L1 levels *via* flow cytometry. Data were shown as mean ± SD ($n = 3$). $^{***}P < 0.001$, $^{****}P < 0.0001$. ns, not significant.

days (Fig. 1F), indicating that it had good stability and was suitable as a carrier for drug delivery.

The intracellular uptake and distribution of nanocarriers reflected their drug delivery capabilities [15]. Various tumor cells, including breast cancer cells 4T1, highly expressed laminin receptors, while PEGCG had a high affinity for laminin receptors in 4T1 cells and could actively target the tumor cells (Fig. 2A and Fig. S2 in Supporting information) [16]. In the targeting assay, for 4T1 cells, the red fluorescence signal of PMD micelles was significantly higher than that of M/D when the blocking agent was not used (Fig. 2A and Fig. S3A in Supporting information). Pre-treatment of cancer cells with PEGCG or laminin receptor antibody 67LR significantly reduced the cellular uptake of PMD micelles, resulting in signal intensity similar to that of MET/DOX mixture (M/D) group. Due to the low expression of laminin receptor in normal cells [17], PMD micelles and M/D had the same red fluorescence signal for L929 cells with or without blocking agent (Fig. 2B and Fig. S3B in Supporting information). These results suggested that the PEGCG endowed PMD micelles with targeting ability.

Some chemotherapeutic agents including DOX could induce ICD in tumor cells and release damage-associated molecular patterns (DAMPs) such as calreticulin (CRT), high mobility group protein B1 (HMGB1) [18,19], which could activate monocytes/macrophages to release pro-inflammatory factors, further regulate the function of endothelial cells and cancer cells [20]. As shown in Fig. 2D, the CRT exposure of DOX, M/D and PMD micelles were significantly higher than that of the control group, MET and PM micelles, especially PMD micelles could induce more CRT exposure. When ICD occurred in tumor cells, the intracellular HMGB1 was released to the extracellular area and cleared through PBS washing. Therefore, the green fluorescence signal of HMGB1 in PMD micelles was the weakest compared with other groups (Fig. 2C), indicating that more HMGB1 was released out of cells. When immature DCs transformed into mature DCs through DAMPs stimulation, mature DCs as antigen-presenting cells could present antigens to T lymphocytes [21]. As shown in Fig. 2E and Fig. S4 (Supporting information), the proportion of mature DCs in MET and PM micelles was significantly lower than that of the DOX, M/D and PMD micelles. Due to the active targeting effect of PEGCG, PMD micelles could allow more DOX to enter tumor cells to induce ICD and release DAMPs, thereby stimulating more immature DCs to transform into mature DCs.

MET could down-regulate the expression of PD-L1 through activating adenosine 5′-monophosphate activated protein kinase (AMPK), and phosphorylation of AMPK (p-AMPK) was an indicator of AMPK activation [22]. The expression level of p-AMPK in 4T1 cells was as shown in Fig. S5 (Supporting information), MET, PM micelles and PMD micelles could induce higher levels of p-AMPK. The flow cytometry further quantitatively showed the similar experimental results with higher levels of p-AMPK in PMD micelles-treated 4T1 cells (Fig. 2F and Fig. S6 in Supporting information). Moreover, we evaluated whether PMD micelles could reduce the expression of PD-L1 in TNBC cell line, 4T1 cells which overexpresses PD-L1 [23–25]. As shown in Fig. S7 (Supporting information), the expression of PD-L1 was attenuated after PMD micelles or MET intervention. In addition, the changes in PD-L1 levels evaluated using flow cytometry showed that the expression of PD-L1 in 4T1 cells treated with PMD micelles, compared with the control group, was significantly reduced (Fig. 2G and Fig. S8 in Supporting information). In conclusion, the above results demonstrated that PMD micelles could be efficiently down-regulate PD-L1 expression through activating AMPK.

The results of cytotoxicity of DOX, MET and PMD micelles *in vitro* showed that the viability of L929 cell and 4T1 cells exceeded 80% at 80 μg/mL of PM micelles concentration, indicating that PM micelles as nanocarrier was not toxic to normal cells and tumor cells (Fig. S9A in Supporting information). MET has been shown antitumor effects, albeit in a limited capacity [26]. As shown in Fig. S9B (Supporting information), the viability of 4T1 cells incubated with MET (32 μg/mL) was less than 80%, which proved that MET had an inhibitory effect on tumor cells, but had no effect on normal cells. As a commonly used chemotherapeutic drug, DOX had obvious inhibitory effect on tumor cells even at lower concentrations. As shown in Fig. S9C (Supporting information),

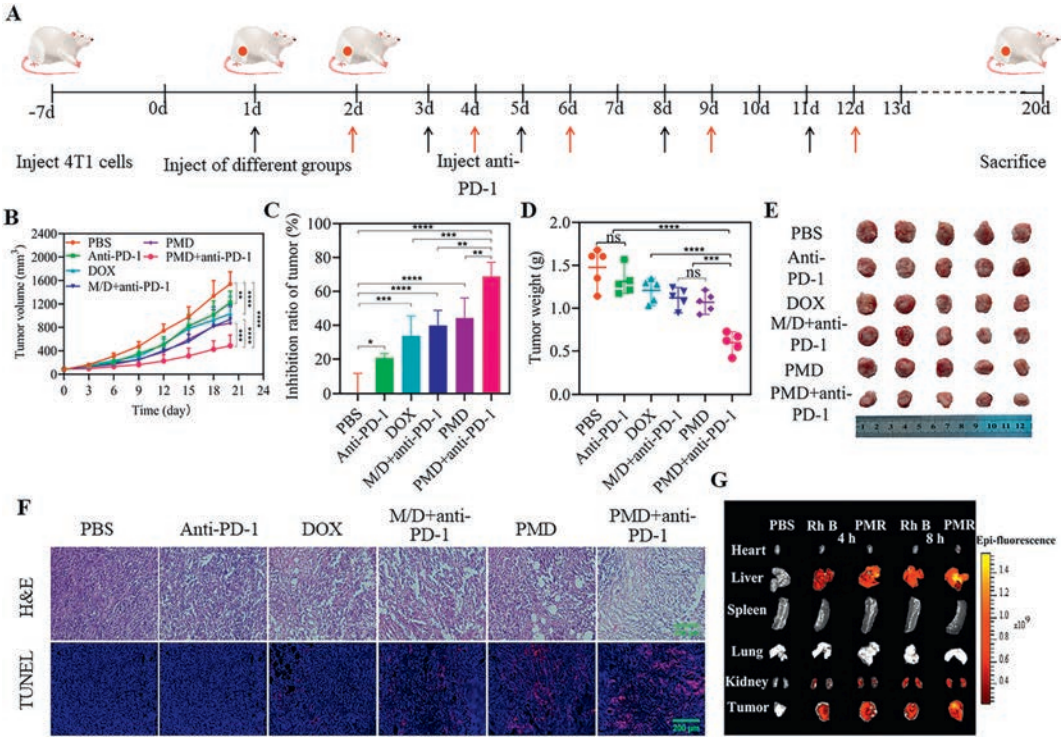

Fig. 3. Anti-tumor effect of PMD micelles combined with anti-PD-1 antibody *in vivo*. (A) Schematic diagram of animal experimental design. (B) Tumors volumes of each group during the treatment. (C) The final tumors inhibition rate and (D) tumors weight of each group during the treatment. (E) Photos of dissected tumors after the 20-day treatment. (F) H&E and TUNEL staining of the corresponding tumor tissues obtained after different treatments. Scale bar: 200 μm. (G) Fluorescence imaging of the major organs and tumors. Data were shown as mean ± SD ($n = 5$). $^{*}P < 0.05$, $^{**}P < 0.01$, $^{***}P < 0.001$, $^{****}P < 0.0001$.

the cytotoxicity of DOX and PMD micelles on 4T1 cells exhibited a concentration-dependent manner. When the DOX concentration reached 7.8 μg/mL, the cell viability dropped to 50%. However, the half-maximal inhibitory concentration (IC_{50}) of PMD micelles was significantly lower than that of free DOX (Fig. S9D in Supporting information). PMD micelles had higher cytotoxicity even at the same DOX concentration due to the targeting effect of PEGCG on laminin receptor of tumor cells and the synergistic antitumor effect of MET. The dead/living assay showed that PMD micelles could induce more tumor cell death compared with free DOX (Fig. S9E in Supporting information), followed by the M/D group. PM micelles and MET hardly showed tumor cell death due to less cytotoxicity. The apoptosis of each group was analyzed by flow cytometry (Figs. S9F and S10 in Supporting information), the results confirmed the enhanced anticancer activity of PMD micelles, and PMD micelles had the highest proportion of apoptotic tumor cells.

Using the 4T1 orthotopic tumor bearing model, PMD micelles combined with anti-PD-1 showed better anti-tumor effect *in vivo*. All animal experiments were approved by the Animal Ethics Committee of Hubei University of Technology. Schematic diagram of 4T1 mice therapy was shown in Fig. 3A. Mice were subcutaneously inoculated with 4T1 cells. 4T1 orthotopic tumor bearing mice were randomly divided into 6 groups and gave treatments when the tumor size reached to 100 mm^3, then the mice were euthanized 20 days after treatment. As shown in Figs. 3B, D and E, compared with the PBS group, the tumor growth rate of the mice treated with anti-PD-1 or PMD micelles was only slowed to a certain extent, but the tumor volume of the mice in the combined PMD micelles + anti-PD-1 group was significantly reduced, and its tumor inhibition rate was 68.8%, which was significantly higher than that of other treatment groups (Figs. 3C and D). From the results of hematoxylin and eosin (H&E) staining, compared with other treatment groups, tumor tissues treated with PMD micelles + anti-PD-1 revealed extensive tumor cell sparseness, deformation and nuclear condensation (Fig. 3F). In addition, the degree of tumor cell apoptosis assessed by the transferase-mediated nick and labeling technique (TUNEL) staining was shown in Fig. 3F. PMD micelles and anti-PD-1 group showed significantly more red fluorescence signal than other treatment groups, indicating that the combined administration could inhibit tumor growth by inducing more tumor cell apoptosis.

The biodistribution of PM micelles loaded with Rhodamine B (PMR) in the 4T1 tumor bearing mice was shown in Fig. 3G and Fig. S11A (Supporting information). The results presented that PM micelles significantly prolonged the circulation time of Rhodamine B, and enhanced tumor targeting through PEGCG mediated targeting and the enhanced permeability and retention (EPR) effects [7]. After 4 h, the accumulation ratio of PMR micelles in tumor/liver and liver/kidney was higher than that of free Rhodamine B (Fig. S11B in Supporting information), indicating that Rhodamine B and PMR micelles were metabolized by the liver and excreted by kidney. At 8 h, in addition to a significant increase in the accumulation of PMR micelles in the kidney, stronger fluorescence signal was observed in the liver and tumor, indicating that PMR micelles was primarily captured by the liver and excreted by the kidney, and was easy to accumulate in the tumor. In contrast, the fluorescence of free Rhodamine B was weaker. At 8 h, only the fluorescence signal in the liver increased significantly compared with that of at 4 h, but the accumulation of Rhodamine B in the tumor was not increased. These results suggested that PMR micelles could enhance tumor targeting *in vivo*. *In vivo* safety of PMD micelles was shown in Fig. S12 (Supporting information), the results of the weight of the mice, the liver injury markers alkaline phosphatase (ALT) and aspartate transaminase (AST) and H&E staining of major organs (heart, liver, spleen, lung and kidney) all proved that PMD micelles had good biocompatibility.

Next, we elucidated the best effect of combined therapy group to inhibit tumor growth through activating the antitumor im-

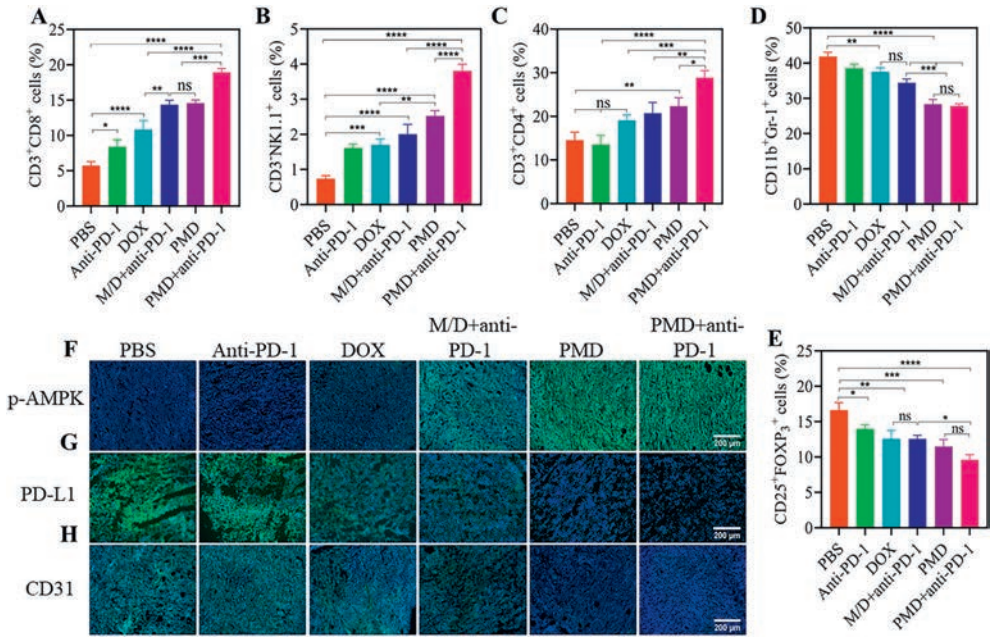

Fig. 4. Regulation of PMD micelles on tumor immune microenvironment. (A) Quantification of the $CD8^+$ T cells. (B) NK cells and (C) $CD4^+$ T cells in tumor tissues. (D) Quantification of MDSCs and (E) Tregs in tumor tissues. (F) Immunofluorescence staining of p-AMPK, (G) PD-L1 and (H) CD31. Scale bar: 200 μm. Data were shown as mean ± SD ($n = 3$). $^*P < 0.05$, $^{**}P < 0.01$, $^{***}P < 0.001$, $^{****}P < 0.0001$.

mune effect and remodeling tumor immune-suppressive microenvironment. More importantly, unlike antibody-based ICIs that acted through the conformation blocking membrane PD-L1, the introduction of MET endowed PMD micelles with the ability to reduce PD-L1 expression in tumor cells, thereby effectively awakening the host's immune system, then restore the function of T lymphocytes.

As main anti-tumor immune cells, $CD8^+$ T cells can secrete interferon-γ (IFN-γ), tumor necrosis factor (TNF-α) and granzyme B (GzyB), thereby playing a role in killing tumor cells [27,28]. Natural killer (NK) cells, as important immune cells, are closely related to immune regulation and anti-tumor effects *in vivo* [29]. Here, the proportion of $CD8^+$ T cells and NK cells in the tumor tissue of tumor-bearing mice treated with PMD micelles + anti-PD-1 was significantly increased (Figs. 4A and B, Figs. S13 and S14 in Supporting information), and the release of GzyB, TNF-α and IFN-γ and were promoted (Figs. S15 and S16 in Supporting information). Meanwhile, PMD micelles + anti-PD-1 could significantly increase the proportion of infiltrating $CD4^+$ T cells compared with phosphate buffer saline (PBS) group (Fig. 4C and Fig. S17 in Supporting information). These results indicated that PMD micelles could increase the antitumor effect by increasing the proportion of tumor-infiltrating T cells and NK cells. DAMPs, such as CRT, were captured by immature DCs and induced transformation into mature DCs, thereby promoting the proliferation of T and NK cells [30,31]. As shown in Figs. S18–S20 (Supporting information), the results *in vivo* proved that they were consistent with the results *in vitro*. Immunosuppressive cells, including MDSCs and Tregs, existed in the tumor, which could reduce the release of cytokines by inhibiting the proliferation and activity of T cells and NK cells, enabling tumor cells to achieve the purpose of immune escape [32]. Studies had shown that EGCG not only had anti-inflammatory and antioxidant effects, but also inhibited the activity of Tregs through inducing apoptosis of MDSCs, thereby improving the tumor immunosuppressive microenvironment [33]. The infiltration of MDSCs and Tregs in tumor tissues was shown in Figs. 4D and E, Figs. S21 and S22 (Supporting information), PMD micelles and PMD micelles + anti-PD-1 could significantly reduce the infiltration of MDSCs and Tregs due to the effect of PEGCG, which could restore the activity of T cells and NK cells and enhanced anti-tumor effect. Furthermore, the results of immunofluorescence staining in activating AMPK and reducing PD-L1 *in vivo* experiment were shown in Figs. 4F and G, the p-AMPK green fluorescence signal in tumor tissue of tumor-bearing mice treated with M/D + anti-PD-1 was significantly increased. Since PMD micelles + anti-PD-1 group had higher AMPK phosphorylation, which could inhibit the expression of PD-L1, so the expression of PD-L1 showed the contrary trend. Otherwise, EGCG also could inhibit the angiogenesis of tumor tissue through reducing the expression of vascular endothelial growth factors (VEGF) in tumor cells [34]. In this paper, the vascular distribution of tumor tissue was shown in Fig. 4H, the tumor vascular distribution of PMD micelles groups were significantly reduced due to the presence of PEGCG, indicating PMD had a good anti-tumor angiogenesis effect.

In conclusion, PMD micelles based on the self-assembly of the immune adjuvant MET and the actively targeted PEGCG could integrate chemotherapy and immunotherapy for enhancing therapy effect of TNBC. PMD micelles could induce DCs maturation by inducing ICD of DOX, promoting T cells and NK cells proliferation, thus releasing large amount of cytokines. Meanwhile, PMD micelles also restored the activity of T cells and NK cells by reducing the infiltration of immunosuppressive cells such as MDSCs and Tregs in the tumor microenvironment. More importantly, PMD micelles could down-regulate the expression of PD-L1 by activating AMPK in 4T1 cells, then restored the killing effect of T cells on tumors to prevent immune escape. In view of these findings, when PMD was combined with ICIs (such as anti-PD-1) as therapeutic strategy of TNBC, PMD micelles could remedy the shortcomings of antibody-based ICIs immunotherapy, provide synergistic effect and enhance antitumor effects.

Declaration of competing interest

The authors declare that they have no known competing financial interests or personal relationships that could have appeared to influence the work reported in this paper.

Acknowledgments

We gratefully acknowledge the projects of the National Key Research and Development Program (No. 2021YFA0716702), the National Natural Science Foundation of China (Nos. 61805122, 22022404 and 22074050) and Green Industry Science and Technology Leading Project of Hubei University of Technology (No. XJ2021003301), the National Natural Science Foundation of Hubei Province (No. 2022CFA033), it was supported by Chinese Society of Clinical Oncology (CSCO) supported by Jiangsu Hengrui Cancer Research Foundation (No. YHR2019–0325), supported by the Fundamental Research Funds for the Central Universities (No. CCNU22QN007), and supported by the Opening Fund from the Jiangsu Key Laboratory of Medical Optics, Suzhou Institute of Biomedical Engineering and Technology (No. JKLMO202203), supported by the Key Laboratory of Optic-electric Sensing and Analytical Chemistry for Life Science, MO (No. M2022–5).

Supplementary materials

Supplementary material associated with this article can be found, in the online version, at doi:10.1016/j.cclet.2023.108536.

References

[1] (a) P.S. Hegde, D.S. Chen, Immunity 52 (2020) 17–35;
(b) S. Dong, B. Liu, S. Hu, et al., Cancer Med. 11 (2022) 4297–4309;
(c) Y. Song, Y. Huang, F. Zhou, J. Ding, W. Zhou, Chin. Chem. Lett. 33 (2022) 597–612;
(d) R. Chen, P. Ouyang, L. Su, et al., Chin. Chem. Lett. 33 (2022) 4610–4616;
(e) Z. Li, J. Huang, T. Du, et al., Chin. Chem. Lett. 33 (2022) 2496–2500;
(f) P. Lan, H. Chen, Y. Guo, et al., Nano Lett. 22 (2022) 4741–4749;
(g) Q. Zhao, W. Zhang, Z. Ning, et al., PLoS One 9 (2014) e93103.
[2] (a) H. Yao, J. Lan, C. Li, et al., Nat. Biomed. Eng. 3 (2019) 306–317;
(b) Y. Liu, M. Zheng, Z. Ma, et al., Chin. Chem. Lett. 34 (2023) 107762;
(c) Q. Xie, P. Zhang, Y. Wang, W. Mei, C. Zeng, Front. Oncol. 12 (2022) 958720.
[3] (a) Q. Luo, Y. Zhang, Z. Wang, et al., Chin. Chem. Lett. 33 (2022) 3497–3501;
(b) J. Gao, H. Zhang, F. Zhou, et al., Chin. Chem. Lett. 32 (2021) 1929–1936;
(c) H. Wan, B. Xu, N. Zhu, B. Ren, Tumor J. 106 (2020) 55–63.
[4] P. Sharma, S. Hu-Lieskovan, J.A. Wargo, A. Ribas, Cell 168 (2017) 707–723.
[5] N. Rufo, A.D. Garg, P. Agostinis, Trends Cancer 3 (2017) 643–658.
[6] L. Fu, X. Ma, Y. Liu, Z. Xu, Z. Sun, Chin. Chem. Lett. 33 (2022) 1718–1728.
[7] N. Yongvongsoontorn, J.E. Chung, S.J. Gao, et al., ACS Nano 13 (2019) 7591–7602.
[8] M. Khoobchandani, K. Katti, A. Maxwell, W.P. Fay, K.V. Katti, Int. J. Mol. Sci. 17 (2016) 316.
[9] M. Daugan, A. Dufay Wojcicki, B. d'Hayer, V. Boudy, Pharmacol. Res. 113 (2016) 675–685.
[10] W. Xiong, Y. Gao, W. Wei, J. Zhang, Trends Cancer 7 (2021) 837–846.
[11] S. Verdura, E. Cuyas, B. Martin-Castillo, J.A. Menendez, Oncoimmunology 8 (2019) e1633235.
[12] (a) Y. Xu, C. Li, X. Ma, et al., Proc. Natl. Acad. Sci. U. S. A. 119 (2022) e2209904119;
(b) L. Tu, C. Li, X. Xiong, et al., Angew. Chem. Int. Ed. 62 (2023) e202301560.
[13] P. Schmid, S. Adams, H.S. R.ugo, et al., N. Engl. J. Med. 379 (2018) 2108–2121.
[14] Y. Fujiwara, A. Mittra, A.R. N.aqash, N. Takebe, Cancer Drug Resist. 3 (2020) 252–275.
[15] (a) Y. Xu, C. Li, J. An, et al., Sci. China Chem. 66 (2023) 155–163;
(b) C. Li, Y. Xu, L. Tu, et al., Chem. Sci. 13 (2022) 6541–6549.
[16] M. Kumazoe, K. Sugihara, S. Tsukamoto, et al., J. Clin. Invest. 123 (2013) 787–799.
[17] S.C. Hsu, N.P. Wu, Y.C. Lu, Y.H. Ma, Pharmaceutics 14 (2022) 1523–1537.
[18] C. Xia, M. Li, G. Ran, et al., J. Control. Release 335 (2021) 557–574.
[19] T. Qin, X. Xu, Z. Zhang, et al., Nanotechnology 31 (2020) 365101.
[20] S. Pahlavanneshan, A. Sayadmanesh, H. Ebrahimiyan, M. Basiri, J. Immunol. Res. 2021 (2021) 9912188.
[21] J. Zhou, G. Wang, Y. Chen, et al., J. Cell. Mol. Med. 23 (2019) 4854–4865.
[22] L.E. M.unoz, L. Huang, R. Bommireddy, et al., J. Immunother. Cancer 9 (2021) e002614.
[23] M.S. Carlino, J. Larkin, G.V. Long, Lancet 398 (2021) 1002–1014.
[24] K. Mediratta, S. El-Sahli, V. D'Costa, et al., Cancers 12 (2020) 3529 Basel.
[25] C. Robert, Nat. Commun. 11 (2020) 3801.
[26] J. Xue, L. Li, N. Li, et al., Eur. J. Pharmacol. 859 (2019) 172541.
[27] S. Cai, Z. Chen, Y. Wang, et al., Theranostics 11 (2021) 1970–1981.
[28] F. De Benedetti, G. Prencipe, C. Bracaglia, E. Marasco, A.A. Grom, Nat. Rev. Rheumatol. 17 (2021) 678–691.
[29] S.J. Judge, W.J. Murphy, R.J. C.anter, Front. Cell. Infect. Microbiol. 10 (2020) 49.
[30] X. Gao, H. Huang, C. Pan, et al., Cancers 14 (2022) 4715–4730.
[31] Z. Gong, M. Chen, J. Miao, et al., J. Immunol. Res. 2022 (2022) 8802004.
[32] L. Ai, S. Mu, C. Sun, et al., Mol. Cancer 18 (2019) 88.
[33] P. Serafini, S. Mgebroff, K. Noonan, I. Borrello, Cancer Res. 68 (2008) 5439–5449.
[34] P. Deng, C. Hu, Z. Xiong, et al., Cancer Manag. Res. 11 (2019) 2425–2439.